Differential Reactivity of Copper- and Gold-Based Nanomaterials Controls Their Seasonal Biogeochemical Cycling and Fate in a Freshwater Wetland Mesocosm

Astrid Avellan, Marie Simonin, Steven M Anderson, Nicholas K Geitner, Nathan Bossa, Eleanor Spielman-Sun, Emily S Bernhardt, Benjamin T Castellon, Benjamin P Colman, Jane L Cooper, et al.

Article

Differential Reactivity of Copper- and Gold-Based Nanomaterials Controls Their Seasonal Biogeochemical Cycling and Fate in a Freshwater Wetland Mesocosm

Astrid Avellan, Marie Simonin, Steven M. Anderson, Nicholas K. Geitner, Nathan Bossa,
Eleanor Spielman-Sun, Emily S. Bernhardt, Benjamin T. Castellon, Benjamin P. Colman, Jane L. Cooper,
Mengchi Ho, Michael F. Hochella, Jr., Heileen Hsu-Kim, Sayako Inoue, Ryan S. King,
Stephanie Laughton, Cole W. Matson, Brittany G. Perrotta, Curtis J. Richardson, Jason M. Unrine,
Mark R. Wiesner, and Gregory V. Lowry*

Cite This: https://dx.doi.org/10.1021/acs.est.9b05097

Read Online

ACCESS | 📊 Metrics & More | 📄 Article Recommendations | ⓈⒾ Supporting Information

ABSTRACT: Reliable predictions of the environmental fate and risk of engineered nanomaterials (ENMs) require a better understanding of ENM reactivity in complex, biologically active systems for chronic low-concentration exposure scenarios. Here, simulated freshwater wetland mesocosms were dosed with ENMs to assess how their reactivity and seasonal changes in environmental parameters influence ENM fate in aquatic systems. Copper-based ENMs (Kocide), known to dissolve in water, and gold nanoparticles (AuNPs), stable against dissolution in the absence of specific ligands, were added weekly to mesocosm waters for 9 months. Metal accumulation and speciation changes in the different environmental compartments were assessed over time. Copper from Kocide rapidly dissolved likely associating with organic matter in the water column, transported to terrestrial soils and deeper sediment where it became associated with organic or sulfide phases. In contrast, Au accumulated on/in the macrophytes where it oxidized and transferred over time to surficial sediment. A dynamic seasonal accumulation and metal redox cycling were found between the macrophyte and the surficial sediment for AuNPs. These results demonstrate the need for experimental quantification of how the biological and chemical complexity of the environment, combined with their seasonal variations, drive the fate of metastable ENMs.
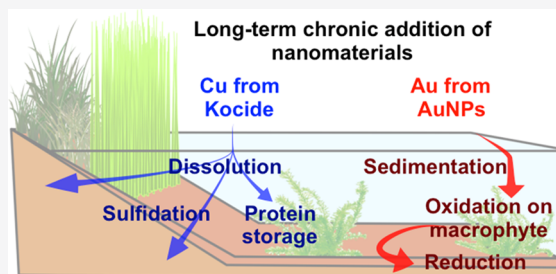
INTRODUCTION

Experimental assessments of the behavior of engineered nanomaterials (ENMs) in complex environments using chronic, low-dose exposures are needed to inform predictions of the ecological risks associated with their uses. Large-scale aquatic mesocosms are a valuable tool for studying the fate of ENMs in the environment.[1,2] They provide realistic information about behavior, transformation, and impact of contaminants in a comprehensive experiment.[3]

The majority of the early mesocosm studies used relatively high-concentration one-time pulse additions of ENMs to enable tracking their fate and to observe system changes. It is now known that high particle concentrations influence their sedimentation, dissolution, exposure routes, and ecosystem impacts that may ultimately occur. For instance, when compared to chronic low-concentration additions, pulse additions using higher ENM concentrations result in homoaggregation that affects the resulting distribution of ENMs[4] and subsequently overestimates the short-term effect of ENMs while underestimating their long-term accumulation and impacts.[5] Thus, the representativeness of the ENM's

release scenarios also depends on the scenario of exposure of the ENMs into aquatic systems.[4−8]

The freshwater mesocosms used here mimic a wetland ecosystem containing several environmental compartments including the water column with relevant aquatic plants, organic-rich floc at the sediment−water interface, and upland soil with terrestrial plants. When ENMs enter the water column, several transformations modulate their persistence in the water column. These transformations can be physical (aggregation, agglomeration, and sedimentation) and/or chemical (dissolution, sulfidation, oxidation, and reduction).[9,10] Environmental factors (ENM concentration, pH, ionic strength, oxygen and sulfide availability, anions concentrations, and type and concentration of organic matter)[11,12] and/or biological processes (adsorption of
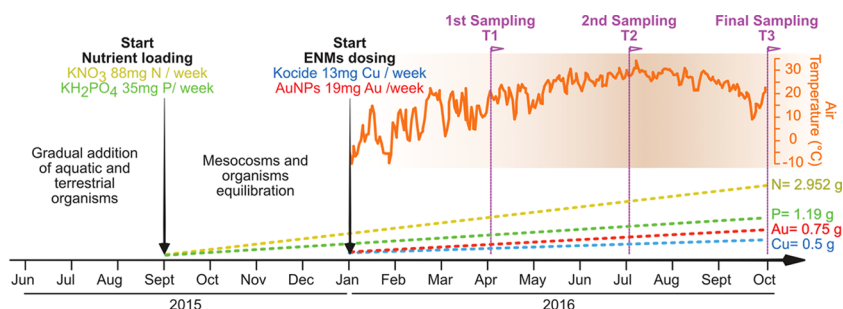
Figure 1. Timeline of the experiment, including dosing and different sampling events. T1, T2, and T3 stand for sampling time points 1, 2, and 3 of the experiment (respectively, 3, 6, and 9 months after ENM dosing started).

biomacromolecules, organic acids, and chelators)[13−15] have been shown to influence these transformations. In addition, in open ecosystems, all of these parameters will vary seasonally[16] and with the level of biological activity[17] and productivity of the ecosystem,[18,19] underlying the need for long-term mesocosm experiments to accurately capture ENM fate in aquatic ecosystems.

The persistence of ENMs in the water column is a key parameter in the assessment of their fate and their transformation products. In particular, ENM dissolution and subsequent ion release can lower the overall persistence of ENMs in the water column, while increasing dissolved species of ENM constituent elements. In comparison to ENM dissolution, more stable ENMs may rapidly be removed from the water column and become associated with sediment,[20] likely decreasing the distribution of metal to other environmental compartments,[9] changing the affinity for ligands and surfaces,[21] and affecting exposure routes for organisms[22] and overall metal bioavailability.[23]

Although it is clear that ENM properties, biological activity, and environmental conditions will influence ENM persistence and transformation, the complexity and seasonal variability of these factors present substantial challenges for predicting ENM fate in these systems. This complexity underlines the importance of mimicking real ecosystems to more accurately reflect both the response of ecosystems to ENM exposure and the (bio)transformations they will undergo.

Thus, this work aimed to assess the fate of ENMs with different dissolution potentials in outdoor simulated freshwater wetlands. Experiments were conducted over 9 months and under high and low nutrient status. These were used to probe the influence of seasonal variations in water quality parameters and biology activity on the ENMs fate. Two different ENMs were tested: (1) Kocide, a nano-Cu(OH)$_2$-based agricultural fungicide that dissolves completely in a few days in mesocosm water[24] and (2) AuNPs, a nanoparticle (NP) resistant to (oxidative) dissolution in (ligand-free[15]) water.[25] Wetland mesocosms established with ambient or enriched nutrients (N, P, and K) were chronically exposed to low concentrations of these ENMs for 9 months. The seasonal and nutrient-induced impacts on water quality parameters were tracked weekly, and ENM fate and transformations were recorded every 3 months by measuring the mass and speciation of the metal in different compartments of the mesocosms. The aim was to test the hypothesis that (i) copper particles in the Kocide formulation, which will dissolve relatively quickly, will accumulate in different sinks of the wetland, while AuNPs will remain in the water column longer as particulate forms and that (ii) environmental conditions, such as seasonal fluctuations, ligand

abundance, pH, and redox gradients, will modify the chemical stabilities of these ENMs.

■ MATERIALS AND METHODS

Mesocosm Setup. In June 2015, 18 outdoor wetland mesocosms were established in the Duke Forest, a research facility located in Durham, NC. The mesocosms are large boxes (dimensions: 3.66 × 1.22 × 0.81 m^3) containing a permanently flooded zone (aquatic zone), a periodically flooded zone (transition zone), and a rarely flooded zone (upland zone) (see Figure S1). The mesocosm setup is detailed in the Supporting Information (SI) (Mesocosm Setup section) and in previous studies using this facility.[15,19,26] The boxes were inoculated with different plant and animal species between June and September 2016. Details about the plant species introduction were described earlier;[19] this can be found in the SI, section "Mesocosms Setup". Each box was randomly assigned to a combination of an ENM and a nutrient status with three replicates for each of six treatments: control−ambient nutrient, control−nutrient enriched, AuNPs−ambient nutrient, AuNPs−nutrient enriched, Kocide−ambient nutrient, and Kocide−nutrient enriched. The nutrient loading began in September 2015, and ENM dosing began in January 2016 (Figure 1).

NP Synthesis, Characterization, and Dosing. Citrate-coated gold nanoparticles (AuNPs) were synthesized following a previously established protocol.[27] AuNP average primary diameter, assessed by transmission electron microscopy, was 11.9 ± 1.2 nm. The Cu-based ENM is a commercially available pesticide, sold as a powder (KOCIDE 3000, DuPont, Wilmington, DE).[28] Kocide 3000 contains ~45% Cu(OH)$_2$. Previous size fractionation studies of Cu from Kocide in water found that 100% of Cu species were below 0.45 μm, with 20% passing through a 0.1 μm filter.[29] Kocide also contains 1−5% of (undefined) clays, 5−10% 2-propenoic acid, and 38.9−47.9% of "other proprietary ingredients".[28] These organic phases may influence ENM fate once released in the environment.[29−31] Because of their increased use, it is likely that both these ENMs will someday reach a freshwater system.

Weekly additions of ENMs were performed over 273 days (39 weeks). The doses of AuNPs and Kocide were intentionally made as low as possible to simulate a chronic low-dose release scenario. The concentration used for Kocide simulated runoff from field application, as described in Simonin et al.[19] The amount of Kocide reaching a wetland over 9 months has been estimated to be 500 mg, based on manufactured recommend application rates, the typical ratio between cultivated land and surrounding wetland area, and a typical rate of loss of agrochemicals from surface soils. The

initial [Cu] in the mesocosm water before starting the NP dosing was $1.48 \pm 0.93 \mu g L^{-1}$. A variable dosing rate was used (i.e., more initially followed by lower concentrations) for the Cu to be detectable at T0 and in the initial quarter of sampling despite the initial Cu background. Inflows of agricultural runoff are episodic, occurring at times of high rainfall, so this scenario is not atypical. Kocide was thus first spiked (347 mg), and then was added weekly at 34.67 mg, representing a cumulative Cu dose of 500 mg after 9 months.

AuNPs were chosen with initial assumptions that they could be an inert particle tracer, as suggested in prior laboratory studies.[15] The dosing regime was designed to ensure that Au would be detectable across time and in various compartments of the mesocosms. The initial [Au] across all of the mesocosms before starting the NPs dosing was $0.42 \pm 0.14 \mu g L^{-1}$. A weekly addition of 19.23 mg of Au as AuNPs was applied to represent a cumulative dose of 750 mg.

An ENM concentrate was mixed with 1 L of mesocosm water and dispersed after sonication throughout the entire aquatic zone below the water surface. Control mesocosms were treated with the same volume of mesocosm water without ENM addition.

Water under ambient and enriched nutrient status was sampled from control mesocosms in September 2016 to characterize NP ζ potential and hydrodynamic diameter using a Zetasizer NanoZS (Malvern, U.K.). These water quality parameters can be found in Table S1.

Dissolution of $Cu(OH)_2$ from Kocide (at 1 mg L^{-1}) was measured in situ (directly in these mesocosms) from 4/11/2016 to 4/13/2016, using a Float-ALyzer G2 dialysis membrane (Spectrum Laboratories, Rancho Dominguez, CA) with a molecular weight cutoff of 10 kDa in either Kocide-treated, ambient, or enriched nutrient status as previously described.[24]

Sample Collection. To assess the fate of the two ENMs in the different compartments, three major samplings at a 3 months interval after the ENM addition were performed at time point 1 (T1) on day 90, time point 2 (T2) on day 193, and time point 3 (T3) on day 269 (see Figure 1). Water column samples of 10 mL aliquots were collected, immediately acidified with HNO_3, and stored at 2 °C. Macrophyte *Egeria densa* samples were collected at 3, 6, and 9 months using steel stove pipes of 20 ± 1 cm of diameter to collect macrophyte biomass present in this given volume. At the end of the experiment (9 months), a destructive sampling was done, and all of the plant biomasses were manually sampled from all of the mesocosms. Periphyton was collected from three *E. densa* young stems (7 cm shoot clippings) thoroughly rinsed in 500 mL autoclaved control mesocosm water. Upland soil and sediment (from transition and aquatic zones) were core-sampled using polypropylene tubes. Three cores were collected per zone, and the aquatic and transition zones were separated into floc (top 0.5 cm surficial aquatic sediment), top sediment (0−1 cm below the floc), and deep sediments (1−5 cm below the floc), and then were individually homogenized. Visible plant roots were removed manually, and the transition and upland soils were sieved through a 2 mm mesh. Snail species (*Physella acuta* and *Lymnaea* sp.) were hand-collected (up to $n = 5$ individuals) at T1 and T2, and all of the snail individuals were collected at the end of the experiment (T3). At the end of the experiment, other macroinvertebrates (primarily Odonate nymphs) were collected and separated by species using a net. Eastern mosquitofish (*Gambusia holbrooki*) was sampled by

trapping at T1−T3 ($n = 5$ and 3 individuals per ENM-treated or control mesocosm, respectively), and all of the fish biomasses were harvested using a net at T3. The fish samples were immediately euthanized with tricaine methanesulfonate buffered with bicarbonate and frozen (Duke University Institutional Animal Care and Use Committee protocol # A135-16-06). All solid samples (soils, sediments, flocs, and organisms) were oven-dried at 60 °C, organisms were weighed for biomass, homogenized by grinding, and stored in sealed containers prior to analysis.

Elemental Analysis and Mass Balance Calculation. Pulverized snails, fish, and macroinvertebrate biomass samples were rehydrated prior to acid digestion, while other samples were digested as a dried material. Digestion was carried out as follows: (i) immersion of the sample in HNO_3 (70%, trace metal grade), heated at 100 °C for 30 min, (ii) addition of HCl (30%) to match a 3:1 volume ratio of HNO_3/HCl, heated at 100 °C for 30 min, (iii) dilution to 2% HCl with ultrapure water, and (iv) filtration at $0.45 \mu m$ (except for fish, snails, and macroinvertebrates digestates). All digested samples were analyzed for Cu and Au concentrations by inductively coupled plasma mass spectrometry (ICP-MS) using Agilent (Santa Clara, CA) 7000-series ICP-MS instrumentation. Spike and certified reference material recoveries were $95.6 \pm 14\%$, and detection limits were determined for each element as (mean of three different reagent blanks) + [3 × standard deviation (SD) of 10 replicate analyses of the reagent blank solution]. Element concentration was then expressed as the mass of the metal (mg) per kg of the dried sample.

The volume of water within the mesocosms fluctuated over the course of the experiment as a result of rainfall and evapotranspiration and was calculated for all sampling time points by carefully measuring water levels within each mesocosm. We measured the bulk density (g cm^{-3}) of soil, sediment, and surficial sediment (floc) samples for all cores and then calculated the total mass of each compartment at T1−T3 by multiplying their volume by their measured bulk density. *E. densa* biomass was measured at T3 by harvesting all of the macrophytes and weighing the dried tissues. *E. densa* biomass at T1 and T2 was calculated for each box as described previously[15] following the equation

$$E.\ densa \text{ dry biomass (g)}$$
$$= 49.4 \times E.\ densa \text{ growth rates (mg m}^{-3}\text{ day}^{-1}\text{)}$$
$$+\ 336.2$$

The total biomass of terrestrial plants, macroinvertebrates, fish, snails, and periphyton could not be determined without a destructive harvest and are thus only used for calculations for our final sampling time point (T3).

The total mass of the metal in each compartment was calculated by multiplying the metal concentration in the dried sample by the total dry mass (measured or calculated) of each compartment. The fraction of Au present in each compartment was calculated as the mass of Au in each compartment divided by the total Au masses dosed in the mesocosms over time. For the Kocide treatment, the mass of Cu in each compartment was calculated after subtracting the background Cu naturally present in the control mesocosms. Uncertainties on the metal fractions were calculated using the average of replicates ($n = 3$ mesocosms), following the rules for error propagation for sums or products.[32] Mass recoveries were calculated as the sum of

metal masses measured in all compartments (mass fraction times the total volume or dry mass of that compartment) with respect to the total added mass of Cu or Au.

Water Physical–Chemical Seasonal Variations. The water column was monitored weekly for temperature, turbidity, pH, conductivity (Probe Eureka Manta 2, Austin, TX), anion concentrations NO_3^-, SO_4^{2-}, Cl^-, Br^- (Dionex ICS 2000 ion chromatograph), and metal concentrations Na, Mg, K, Ca, Mn, Fe, Cu, Zn, and Au (ICP-MS, Agilent 7900). Additional continuous measurements of pH and O_2 were done using a EXO1 data probe (YSI, Yellow Springs, OH) over a couple of days to capture daily variations. On a monthly basis, the dissolved organic carbon (DOC) concentration was measured on a Shimadzu TOC-VCPH analyzer with a TNM-1 module and total P on a Beckman DU-64 spectrophotometer. Dissolved oxygen (DO) concentrations (at 15 cm below the water surface) were measured weekly before dawn and at noon using a YSI DO200 or YSI 556. The dissolved CO_2 concentration in the water column was calculated from the CO_2 concentration in a headspace equilibrated with mesocosm water in a closed vessel. The CO_2 concentration in the headspace gas sample was determined using a Shimadzu 17A gas chromatograph using a Tekmar 7050 headspace autosampler.

Chemical Equilibrium Models for Cu Speciation Calculation in the Water Column. Equilibrium copper speciation was estimated for a simplified mesocosm water system using Visual MINTEQ 3.1.[33] The standard input parameters used by the model for all conditions are provided in Table S2 based on the average water parameters over the course of the 9 months experiment. Parameter values used (pH, DOC, O_2, and Cu concentrations) represent the variation measured over the course of the experiments, as presented in Table S3. Ionic strength was calculated from the measured water column components. The Stockholm humic model (SHM) implemented in MINTEQ was used for calculating the complexation of Cu with dissolved organic matter (DOM),[34] with an assumed 10% fulvic acid and 90% humic acid distribution and a ratio of DOM to DOC of 1.65, as previously reported for similar freshwater systems.[35−37] The Cu input to the system was specified as a finite amount of $Cu(OH)_{2(s)}$ solid. Possible solid and dissolved species are specified in Table S4.

Metal Speciation. Copper speciation changes of Cu and Au were tracked in the surficial floc sediment and in *E. densa* at T1 (when metal concentrations were sufficiently high for analysis), T2, and T3. All samples were immediately frozen at −20 °C after harvesting and then stored at −80 °C. Just before measurements, samples were freeze-dried at −53 °C and 2 Pa for 48 h to minimize O_2 exposure, and the dried powders were then ground, pressed into 6 mm pellets, sealed into Kapton tape, and maintained under anoxic conditions to avoid speciation changes. Pellets were analyzed using Au L_{III} edge (11.9 keV) and Cu K edge (8.98 keV) X-ray absorption near-edge structure spectroscopy (XANES) was recorded under 77 K cryostat conditions to avoid beam damage. All spectra were collected at the Stanford Synchrotron Radiation Lightsource beamline 11-2 [using a Si(220) φ = 90° crystal, spot size 5000 × 500 μm^2, and a Canberra 100-element Ge detector] and at the Advanced Photon Source beamline 20-ID [using a Si(110) crystal, spot size 300 × 100 μm^2, and a Vortex Si four-element detector]. For every sample, four to nine XANES spectra were recorded at different locations of the pellets to avoid beam

damage and check for sample homogeneity. Spectra were calibrated using an Au foil (E_0 = 11 911.9 eV) or a Cu foil (E_0 = 8980.5 eV) and merged using SIXPack[38] version 1.2. Spectra normalization and linear combination fitting (LCF) were performed with the Athena software package.[39] The LCF modeling first entailed identification of a reference with the best fit to the data. A second component contribution to the LCF was added to the first one if both (i) its contribution to the model was above 10% (except for Au-CN that had a very intense white line, for which a 3% was chosen) and (ii) the second component reduced the χ^2 and the R-factor values (i.e., quality factors) by more than 20%.

The references used for the linear combination fits along with the provenance and synthesis protocols are presented in the Supporting Information.

■ RESULTS AND DISCUSSION

Water Chemistry Seasonal Variations and NP Persistence. Over the course of the 9 months experiment, the mesocosms underwent seasonal variation, with changes in air temperature (Figure 1), solar radiation, and precipitation (Figure S2A), that led to significant variation in water temperature (from 10 to 35 °C) (Figure 2). The warmest month was July 2016, during the T2 sampling period. The effects of seasonal variation on the water column physicochemical properties were assessed regularly (Figures 2 and S2). While the average water pH remained relatively constant over time (see Figure S2B), diel variations were high (pH ranging from 7 to 10), with a significant daily variation of >1 pH unit (see the example in Figure S3). pH variations are due to O_2 and CO_2 consumption and release by photosynthetic activity and respiration, driven by the abundant biomass of primary producers (algae and *E. densa*) in this system.[40] Indeed, large diel pH, DO, and CO_2 variation in natural macrophyte-rich ponds has been reported in numerous publications,[40−42] where O_2 and CO_2 variations are driven by photosynthesis and respiration. The variation in pH is mainly a consequence of the acidic CO_2 release and uptake during photosynthesis and respiration. This pH variation can also be caused by CO_2 loss by calcification at high pH.[40] Finally, at low CO_2 concentrations, bicarbonate (HCO_3^-) can be used by the primary producers to maintain photosynthesis,[43,44] which will further increase the pH when CO_2 concentrations are low.

Dissolved organic carbon (DOC) increased to a maximum of 27 mg L^{-1} during the spring and declined to 2 mg L^{-1} throughout the summer (Figure 2). This shift in DOC concentration is likely due to both enhanced photolytic and microbial degradation of DOC during the well-lit and warm summer[45] as well as reduced DOC production by the dominant macrophyte *E. densa* during periods of high water temperature and low water oxygen availability.[46] Organic matter is known to influence ENM and soluble metal persistence and mobility in the water column.[14] The concentration of Cu in the water column did decrease when DOC concentrations were lower (at T2 and T3), as shown in Figure 2.

Redox conditions fluctuated daily during the course of the experiment (see the example in Figure S3). Over the course of the summer, the wetland mesocosms became on average more reducing, with dissolved CO_2 concentration increasing, and the greater occurrence of anoxic or low oxygen conditions (Figure 2). Higher demand for alternative terminal electron acceptors
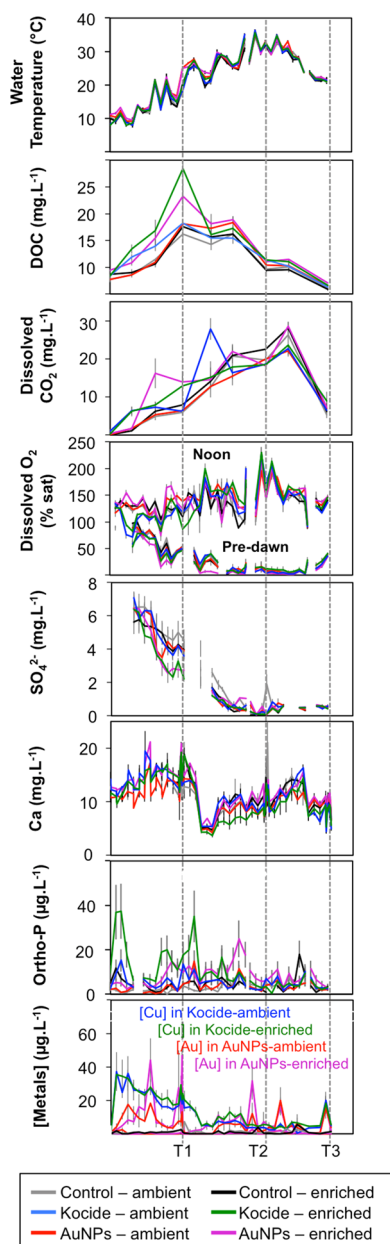
Figure 2. Physicochemical parameter changes over time in mesocosm water with ambient or enriched nutrient status for the different treatments (Kocide or AuNP). T1, T2, and T3 stand for time points 1, 2, and 3 of the experiment (respectively, 3, 6, and 9 months after ENM dosing started).

7.5). As shown in Table S5, ζ potentials (and hydrodynamic diameters) of Kocide (10 mg L^{-1}) were -31.9 ± 6.5 mV (120 $\pm$ 30 nm) and -32.8 ± 1.6 mV (105 $\pm$ 7 nm) under ambient or enriched nutrient status, respectively. For AuNPs, no differences in ζ potential and hydrodynamic size were observed either between ambient nutrient (-13.0 ± 6.2 mV; 10.9 ± 1.4 nm) and enriched nutrient status (-14 ± 1 mV; 11.9 ± 0.2 nm). The ζ potential of these NPs remained negative over a range of pH adjusted from 3 to 12 (with either diluted NaOH or HCl reagents), decreasing from -10 to -35 mV with increasing pH (see Figure S4).

If no differences in hydrodynamic diameter and ζ potential were induced by the nutrient status, seasonal variations of water chemistry may have influenced the dissolution of NPs in the water column in different ways. The average metal concentration in the mesocosm water (Figure 2) was higher for Cu than for Au until T2 of the experiment, likely as a result of the higher initial dosing of Kocide. Nutrient enrichment did not influence either Au or Cu concentrations. Concerning the persistence of Kocide and AuNPs, in vivo tests performed with AuNPs in ambient and enriched control mesocosm water showed no dissolution over the course of 2 weeks.[15] For Kocide, in situ dissolution experiments in the mesocosm water column demonstrated that after 48 h, $60 \pm 8\%$ of the Cu leached out of the dialysis bag in the absence of nutrient addition and $70 \pm 3\%$ in nutrient-enriched conditions[24] (see Figure S5).

Calculated Cu speciation using the Visual MINTEQ v. 3.1 software (details about the models can be found in Tables S2–S4 and S6) indicates that, at equilibrium, 100% of $Cu(OH)_{2(s)}$ should have dissolved. The added Cu should be 100% complexed with dissolved organic matter (Table S6) for the range of pH, DOC, O_2, and Cu concentrations measured in the water column during the 9 months experiment. This is consistent with what has been previously described for Cu in contaminated streams[47] and in line with expectations based on the dissolution rate of Kocide measured in the mesocosms (Figure S5).

Ca and ortho-phosphates are known to affect NP colloidal stability.[48] In this system, the orthophosphate concentration did not correlate with Cu and Au concentrations except for Kocide treatment enriched in nutrients (Table S7) likely because of the low orthophosphate concentrations due to its consumption by *E. densa*. When [Ca] correlated with Cu concentration, it also correlated with the total water volume, indicating that the dissolved Cu concentration, primarily associated with DOM, was mainly affected by dilution effects. In contrast, the Au concentration did not correlate with the water volumes in the mesocosms, likely because of the low Au concentrations in the water column due to its rapid sedimentation. Nevertheless, the Au remaining in the water column was likely in the nanoparticulate form. The differences in dissolution between Kocide and AuNPs in the water column led to contrasting metal persistence in mesocosm water, which also affected their distribution in the different mesocosms compartments.

Cu and Au Differed in Their Recovery and Transfer across Ecosystem Compartments. The masses of Cu and Au in different mesocosm compartments were determined 3 months (T1), 6 months (T2), and 9 months (T3) after the initiation of weekly ENM dosing additions (see Figure S6 and Table S8 for the mass recoveries). The percent recovery for Au in the mesocosms was high for all points of time [(93 $\pm$ 11) to

was apparent, with SO_4^{2-} concentrations falling below detection (DL = 0.01 mg L^{-1}) throughout the summer. Algal blooms during the summer[19] and high *E. densa* densities were contributing to dramatic daily swings in dissolved oxygen concentrations and redox state[40] throughout the mesocosms.

No drastic difference in water chemistry was induced by the addition of nutrients in the mesocosms over the 9 months of experiments, and only a few differences relative to controls were observed in DOC, ortho-phosphates (Figure 2), small variations that had no significant impact on water pH and conductivity (Figure S2B and Table S1). As a result, the ζ potential and hydrodynamic sizes of Kocide and AuNPs in control mesocosm waters were similar under ambient or enriched nutrient status (filtered at 0.45 μm, pH adjusted to
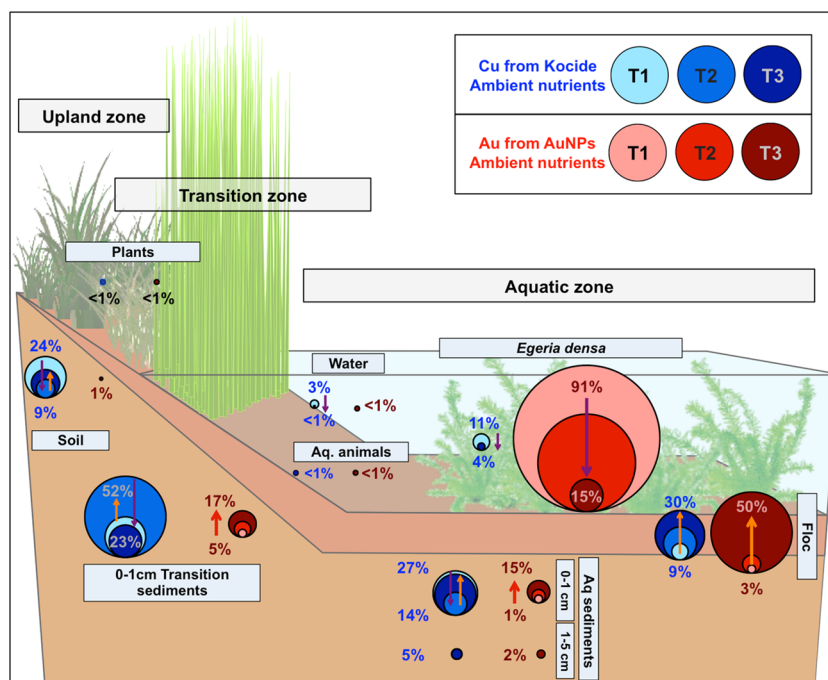
Figure 3. Metal mass distribution for Cu from Kocide (in blue) and Au from AuNPs (in red) in the mesocosms without nutrient addition over time. T1 = 3 months, T2 = 6 months, and T3 = 9 months. Up/down arrows show the trends between each time point. Metal masses were calculated from average concentrations of metal in each compartment and mass of each phase. Note that the floc layer was approximately 0.5 cm thick above the sediments.

$(115 \pm 18)\%$]. For Cu, mass recovery at T1 and T2 was lower [from (58 ± 12) to $(66 \pm 15)\%$] than at T3 ($96 \pm 20\%$ for ambient nutrients and $83 \pm 16\%$ for enriched nutrients). The lower recoveries for Cu at T1 and T2 could be a result of biased sampling due to a heterogeneous distribution of the Cu in the mesocosm, as was observed for CeO_2 NPs in our previous study[26] and/or due to a higher Cu background (in control boxes, [Cu] = 21 ± 2 mg kg^{-1} in the floc and 10.6 ± 2.4 mg kg^{-1} in the sediments) making it challenging to distinguish naturally occurring vs dosed Cu at these earlier time points. It is also worth noting that the Cu concentration in the deep sediments (1−5 cm) was not measured at T1 and T2, while accounting for 5% of the total Cu mass and 2% of Au mass at T3. A part of the unaccounted Cu at these earlier points of time could come from that compartment and could explain the better recovery at T3.

The distribution of the metal recovered within the mesocosms (under ambient nutrient status) was markedly different for Cu compared to Au (Figure 3), indicating that differences in persistence influenced their fates. For all time points, while large quantities (>50%) of Cu transferred into the nonflooded compartments (transition and upland soils), Au was mostly retained (65−90%) in the aquatic compartment associated with *E. densa* or in the floc + aquatic sediment (Figure 3). The lower transfer of Au to the upland regions is similar to what was previously observed with CeO_2 of similar size, which are also relatively stable against dissolution.[26] This difference is a result of the fast (within hours) dissolution of Cu from Kocide in the mesocosm water,[24] making it more concentrated in the water column (Figure 2), more labile, and thus amenable to distribution to the upland and transition zones as water levels fluctuated. However, despite the higher Cu concentration in the soil, the Cu concentration in terrestrial plants did not significantly increase at the end of the

experiment in comparison to the control treatment likely because of uptake regulation of Cu by these terrestrial plant species.[49]

While Cu concentrations in the water column remained higher than Au concentrations (Figure 2), they represented a small percentage of the total added metals. Furthermore, these percentages decreased (for Cu from 3% at T1 to 1% at T3) or remained constant (for Au, ~1%) over time (Figure 3). The differences in Cu and Au concentrations in the water column suggest that aquatic organisms were exposed to different levels of the two metals. Accumulation of Cu and Au in all aquatic animals (fish, snails, and macroinvertebrates) accounted for less than 1% of the total masses of added NPs. Yet, Cu concentrations in the snail *P. acuta* were 45 times higher than in the control treatments (5770 vs 126 mg kg^{-1} dw, respectively) at T3 and 300 times higher than in the AuNPs treatment (in which Au concentration reached 19 mg kg^{-1}). Au accumulation in snails was in accordance with what was previously observed with CeO_2 NPs of similar primary size, at similar mass loadings.[26] Note that the water column of the mesocosms was dominated by *E. densa*, inducing a low light penetration in the water and an oxygen level that dropped near zero at night. As a result, the total biomass of fish, snails, and aquatic insects was at the low end of the range observed in natural systems.[50] The low partitioning of Au and Cu observed in these compartments thus does not necessarily represent those of an ecosystem less dominated by macrophytes, where snails and aquatic insects are more naturally abundant.

Metals Associated with Macrophytes Transfer to the Floc Compartments over Time. The macrophyte *E. densa* was an important reservoir for both NPs, although uptake and assimilation of Au from AuNPs were substantially higher than for Cu from the Kocide treatment. It should be noted that metal measurements were made on unrinsed macrophytes,
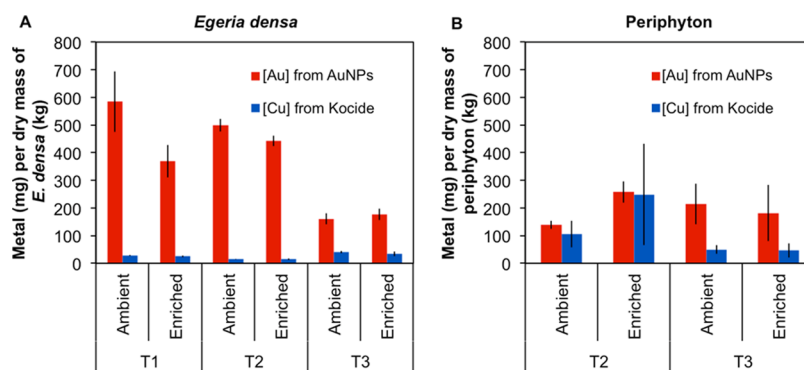
Figure 4. Metal concentration (red: gold and blue: copper) associated with (A) *E. densa* or (B) its periphyton (right). Means and 95% confidence intervals are presented.

which include the metal accumulated within the periphyton that grow on its leaves. Even though ENM suspensions were added weekly during the 9 months of the experiment, the metal concentrations (Figure 4) associated with *E. densa* were constant for Cu and decreased over time for Au. Au concentrations associated with *E. densa* were high, declining from 600 to 150 mg kg^{-1} (Figure 4), representing 90% (at T1) to 15% (at T3) of the total Au added to the system (Figure 3). In comparison, Cu concentrations associated with the macrophytes were significantly lower, ranging 15−40 mg kg^{-1}, representing only 4−11% of the added Cu in the system (Figure 3). This Au association with *E. densa* was much higher than what was observed in prior studies using CeO_2 NPs of similar sizes, dosed simultaneously as the present work in separate mesocosms, that ranged from 5 to 40 mg kg^{-1}.[26]

Au association with *E. densa* was 10−20 times higher than Cu during the full duration of the experiment (Figure 4A). However, the Au and Cu concentrations in the biofilms coating the *E. densa* leaves were only different at T3 and only by a factor of 3−4 (Figure 4B). This indicates that Au was bioaccumulating in the macrophyte tissues and was not simply interacting with the periphyton coating its surface. Indeed, Au or Cu concentrations associated with *E. densa* could not be explained by Au and Cu concentrations in the water column or with their deposition on the macrophyte surface as proxied by Au and Cu concentrations in the biofilm covering the macrophyte surface (absence of correlations between these traits, Figure S7A,B). Au and Cu association with *E. densa* did not correlate with its growth rate either (Figure S7C), indicating that these Au and Cu concentration variations were not due to the generation of a new tissue during plant growth. Altogether, this suggests that a parameter other than exposure or biodilution is affecting Au and Cu uptake into the macrophytes. These large differences of concentration in *E. densa* could be due to a difference in homeostasis between Cu and Au species,[51] and/or in their bioavailability, as discussed later.

The fraction of metal masses associated with *E. densa* decreased over time, and a large fraction of each metal was subsequently transferred into the floc compartment. While *E. densa* was the major sink for Au at T1 and T2, the mass of Au associated with *E. densa* decreased over time, and the aquatic floc became the main reservoir for Au by the end of the experiment (Figures 3B and S6). Snail activity may be one driver of that cycle. While grazing on the macrophyte periphyton and leaves, snails may accumulate the metal and also eliminate it through their excretion and egestion,

potentially leading to metals accumulating in the floc. A complementary hypothesis for the transfer of Au from *E. densa* to floc could be a result of the *E. densa* growth cycle. Over the course of its life cycle, *E. densa* will release dead plant tissues[52] that will accumulate in the floc compartment along with the Au associated with it; while newly grown, younger leaves will have lower metal concentrations. Finally, as described later, the Au association with *E. densa* seems to be strongly related to its speciation. Shifts in water physico−chemical chemistry, as well as the microbial community,[15] could be a driver for these bioavailability changes.

Copper from Kocide Dissociated in the Water Column, while AuNP Transformed at the Plant−Water Interface. The speciation of the Cu and Au was measured in the primary metal sinks of the system (namely, floc and *E. densa*) at T1−T3 (Figure 5). According to the manufacturer,
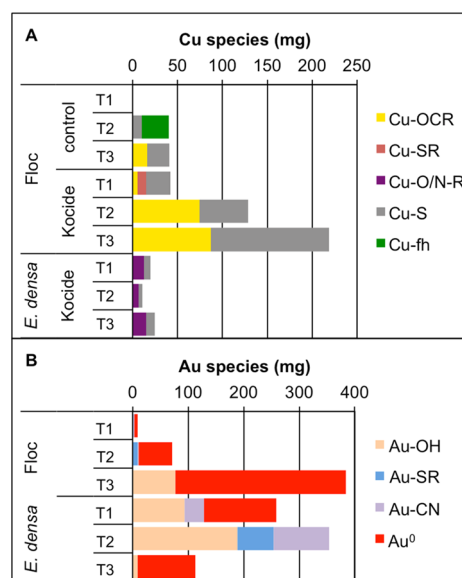

Figure 5. Abundance of the different Cu (A) and Au (B) species in the mesocosm floc and *E. densa* under ambient nutrient status at each sampling event (error estimated at ±10%). Metal species abundances are based on XANES fitting results (see Tables S9, S10 and Figures S8−S10). Cu-OCR: Cu-carboxyl. Cu-SR. Cu-glutathione. Cu-O/N-R. Cu-CopC (protein).[53] Cu-S: Cu-sulfide. Cu-fh: copper sorbed to ferrihydrite. Au-OH: Au-hydroxide. Au-SR: Au-cysteine. Au-CN: Au-cyanide. Au^0: metallic Au. See the Supporting Information (Table S11 and Figure S11) for more details about the reference compound synthesis.

Kocide is a product containing 46.1% $Cu(OH)_2$. Based on its XANES spectra, Cu in Kocide is indeed bound not only to hydroxide but also to hydrogenophosphate-like groups (see Figure S8). While the precise speciation of Cu in the initial Kocide product is proprietary, after being added to the mesocosm water column, the Cu species present in the floc were primarily in a Cu sulfide form and with the remaining copper bound to organic phases. No $Cu(OH)_2$ was measured, indicating a complete dissolution and further transformation of the "nano-Cu" component of the Kocide. The Cu adsorbed on ferrihydrite observed at T2 in the control box was not measured in the Kocide treatment. But by T3, Cu speciation was not different from the naturally occurring Cu species in the mesocosms. The major species associated with *E. densa*, Cu-S, and a Cu-O/N-R[53] suggest a protein storage mechanism for Cu. As described earlier, Cu concentrations associated with *E. densa* were constant over time (Figures 3A and 5A). These results suggest that Cu uptake by the macrophyte is regulated, and/or that a maximum absorption plateau on tissues was reached.[51]

The absence of the $Cu(OH)_2$ from Kocide, the similarity of the Cu species in floc compared to the control, and the protein-like storage of Cu in *E. densa* indicate that the Cu that rapidly dissolved from Kocide[24] subsequently entered the Cu biogeochemical cycle, similarly to naturally occurring copper. These results are different from a previous experiment by our group using similar mesocosms, but at a much higher ENM dose (3 g total over 4 weeks) using different Cu species (CuO NPs and CuS NPs). These higher doses induced a high toxicity of Cu on *E. densa* that affected the biogeochemical cycling of Cu, shifting toward that expected for a heavily Cu-contaminated system.[54] Thus, a much higher fraction (almost 100%) of Cu was associated with Cu-O-R phases during the winter due to a higher amount of organic matter from senescence and dead plant matter. The surficial floc was also likely a more reducing environment, with some Cu reduction to Cu^0 occurring during the summer. Furthermore, despite no clear effect of nutrient addition on the fate of Cu and Au in these wetland mesocosms, we observed a large impact on biota and ecosystem function when nutrients were added along NPs.[19]

Based on the previous work using CeO_2 NPs of different sizes that are relatively stable against dissolution in abiotic water, AuNPs were expected to behave similarly to other nondissolving NPs and to be mainly found in the sediment compartments.[26] However, *E. densa* was the primary sink for Au during the first 6 months of the experiment. The large majority of Au associated with *E. densa* was oxidized at T1 (50%) and T2 (100%) and complexed with -thiol, -hydroxide, and -cyanide (Figure 5B). As we demonstrated earlier, this oxidation is at least partly due to microbial cyanogenic activity in the periphyton covering *E. densa* leaves.[15] The oxidation of AuNP was unexpected since the inert material was intended to be used as an inert tracer for a nanospecific nanoparticle behavior in the mesocosms.[1,15] This unexpected biotransformation was only observed because of the low and chronic AuNP doses added to a biologically active environment with the presence of hydroxide and thiol ligands.[15,55] These local biotransformations of metallic AuNPs into oxidized species made them likely more bioavailable to *E. densa*. This statement is supported by the positive correlation between Au accumulation and oxidized Au species in association with *E. densa* ($r = 0.72$, p-value = 0.096; Figure S12). The higher

toxicity of oxidized Au species compared to that of metallic Au could also explain the correlating impact of Au association with *E. densa* and its altered metabolic and growth rates, as previously reported.[19]

At T3, the fraction and the total mass of oxidized Au associated with macrophytes decreased. This could be explained by a combination of several factors. First, the shift of the system toward a more reduced environment, as indicated by the variation in concentrations of SO_4^{2-}, dissolved O_2, and CO_2 between day and night starting at T2 (Figure 2), may have changed Au speciation from oxidized to reduced species, and thus its bioavailability. Second, a growing snail population may have reduced the biomass of, or modified, the periphyton populations on *E. densa* leaves, lowering the microbial activity responsible for Au biodissolution, and thus its potential for uptake by the macrophyte. Finally, *E. densa* biomass turnover due to the macrophyte senescence−revival cycle in that period, and/or limited growth due to an algal bloom, could have resulted in Au sedimentation.

After flocculation, a fraction of the Au present in the floc (10% at T2 and up to 20% at T3) was oxidized and complexed to -thiol or -hydroxide species. Thiol ligands could come not only from microbial activity[15] but also from dissolved organic carbon molecules (Figure 2). Finally, the presence of metallic Au species in the floc contrasts with the oxidized species abundant in T1 and T2, suggesting some reduction of the oxidized Au. This can be explained by the pH gradient from the water column (pH 7−9, see Figure S2B) to the floc compartment (pH ∼ 6.5, see Figure S13) as well as what was likely a more reduced environment in the sediment surficial floc compartment. It has been shown that Au oxidation state is strongly sensitive to pH and redox variations in these types of environments.[55]

Understanding the Biogeochemical Cycling of Inorganic ENMs is Needed for Accurate Prediction of Their Fate. The diel and seasonal variations in water chemistry along with *E. densa* life cycles were precisely tracked over the course of this 9 months experiment. Large daily variations in pH, O_2, and CO_2 are due to photosynthetic processes and are typical of water bodies dominated by primary producers.[40−42] The shift of the mesocosms toward more reducing conditions at the end of the summer is also consistent with expectations for wetland ecosystems.[56] Thus, the transformation and differential biogeochemical cycling between Cu from Kocide and Au from AuNPs are likely to be representative of their occurrence in freshwater wetland ecosystems.

These results further demonstrate that ENM persistence and dissolution rate influence their mobility and accumulation in different ecosystem compartments. Compared with AuNPs, $Cu(OH)_2$ from Kocide readily dissolved in the water column within hours,[24] was more mobile, accumulated greater in the snails, the transition and the upland sediments, and transferred to the deeper aquatic sediments. This higher potential of Cu for transfer to the soil compartment and the grazers suggests that it may have a different trophic transfer potential from Au. Cu was distributed and transformed similarly to naturally occurring Cu species, i.e., as sulfide minerals, stored in proteins, or ligated with organic phases.

In contrast, AuNPs were more stable against dissolution in water, deposited onto macrophyte surfaces where it was biotransformed and oxidized. This oxidized, more bioavailable Au species correlated well with Au content in *E. densa* tissues.

The accumulation of Au by the macrophyte is likely influenced by several factors like seasonal variation modifying pH and redox potentials, *E. densa* life cycles, and/or grazer activity. While *E. densa* was the major sink for Au during the first 6 months of the experiment, Au masses built up in the floc compartment over time. With seasonal progression, Au transferred from senescent *E. densa* to the floc surficial sediment, where it was further reduced to metallic Au due to pH, and likely redox, gradient changes.

Understanding the ENM properties and processes that drive the impacts and fate of nanomaterials in aquatic environments is crucial.[57] Past studies have shown the importance of ENM behavior model colloidal stability, attachment to surfaces, and dissolution.[22] The present work highlights the complexity of choosing the most appropriate proxy to assess dissolution of ENMs in ecosystems. The prediction of ionic release from reactive, metastable, inorganic ENMs is difficult as it is also influenced by the nature of the environment, their compartmental metal accumulation, the development of the systems over time, and the role of dynamic biological activities. Using dissociation constants in pure water as model inputs for NPs presenting relative dissolution stability may not be an appropriate proxy to capture the behavior and impact of metastable ENMs in the environment.[3,58] Predicting the fate of ENMs in complex ecosystems that are shown to be inert in relatively pure (ligand-free) aqueous systems will require a better understanding of their metastable character, the biotransformations that may occur in each ecosystem sink, and their transfer between compartments.[15,59,60]

■ ASSOCIATED CONTENT

ⓢ Supporting Information
The Supporting Information is available free of charge at https://pubs.acs.org/doi/10.1021/acs.est.9b05097.

Additional information concerning the mesocosm setup, ENM ζ potential, and hydrodynamic diameters, Visual MINTEQ equilibrium models, water chemistry and NP parameters, calculated Cu speciation in the water column, mass balance, Au and Cu speciation and floc pH (PDF)

■ AUTHOR INFORMATION

Corresponding Author
Gregory V. Lowry − Center for the Environmental Implications of Nanotechnology, Durham, North Carolina, and Carnegie Mellon University, Pittsburgh, Pennsylvania; ⓞ orcid.org/0000-0001-8599-008X; Email: glowry@andrew.cmu.edu

Other Authors
Astrid Avellan − Center for the Environmental Implications of Nanotechnology, Durham, North Carolina, and Carnegie Mellon University, Pittsburgh, Pennsylvania; ⓞ orcid.org/0000-0001-6081-4389
Marie Simonin − Center for the Environmental Implications of Nanotechnology, Durham, North Carolina, and Duke University, Durham, North Carolina; ⓞ orcid.org/0000-0003-1493-881X
Steven M. Anderson − Center for the Environmental Implications of Nanotechnology, Durham, North Carolina, Duke University, Durham, North Carolina, and North Carolina State University, Raleigh, North Carolina
Nicholas K. Geitner − Center for the Environmental Implications of Nanotechnology, Durham, North Carolina, and Duke University, Durham, North Carolina; ⓞ orcid.org/0000-0003-4313-372X
Nathan Bossa − Center for the Environmental Implications of Nanotechnology, Durham, North Carolina, Duke University, Durham, North Carolina, and LEITAT Technological Center, Terrassa, Spain
Eleanor Spielman-Sun − Center for the Environmental Implications of Nanotechnology, Durham, North Carolina, and Carnegie Mellon University, Pittsburgh, Pennsylvania; ⓞ orcid.org/0000-0001-9626-2969
Emily S. Bernhardt − Center for the Environmental Implications of Nanotechnology, Durham, North Carolina, and Duke University, Durham, North Carolina
Benjamin T. Castellon − Center for the Environmental Implications of Nanotechnology, Durham, North Carolina, and Baylor University, Waco, Texas; ⓞ orcid.org/0000-0001-8883-076X
Benjamin P. Colman − Center for the Environmental Implications of Nanotechnology, Durham, North Carolina, and University of Montana, Missoula, Montana
Jane L. Cooper − Center for the Environmental Implications of Nanotechnology, Durham, North Carolina, and Duke University, Durham, North Carolina
Mengchi Ho − Center for the Environmental Implications of Nanotechnology, Durham, North Carolina, and Nicholas School of the Environment, Durham, North Carolina; ⓞ orcid.org/0000-0001-6876-9666
Michael F. Hochella, Jr. − Center for the Environmental Implications of Nanotechnology, Durham, North Carolina, Virginia Polytechnic Institute and State University, Blacksburg, Virginia, and Pacific Northwest National Laboratory, Richland, Washington
Heileen Hsu-Kim − Center for the Environmental Implications of Nanotechnology, Durham, North Carolina, and Duke University, Durham, North Carolina; ⓞ orcid.org/0000-0003-0675-4308
Sayako Inoue − Center for the Environmental Implications of Nanotechnology, Durham, North Carolina, and Virginia Polytechnic Institute and State University, Blacksburg, Virginia
Ryan S. King − Center for the Environmental Implications of Nanotechnology, Durham, North Carolina, and Baylor University, Waco, Texas
Stephanie Laughton − Center for the Environmental Implications of Nanotechnology, Durham, North Carolina, and Carnegie Mellon University, Pittsburgh, Pennsylvania
Cole W. Matson − Center for the Environmental Implications of Nanotechnology, Durham, North Carolina, and Baylor University, Waco, Texas; ⓞ orcid.org/0000-0002-6472-9357
Brittany G. Perrotta − Center for the Environmental Implications of Nanotechnology, Durham, North Carolina, and Baylor University, Waco, Texas

Curtis J. Richardson − *Center for the Environmental Implications of Nanotechnology, Durham, North Carolina, and Nicholas School of the Environment, Durham, North Carolina;* ⓘ orcid.org/0000-0002-8373-6587

Jason M. Unrine − *Center for the Environmental Implications of Nanotechnology, Durham, North Carolina, and University of Kentucky, Lexington, Kentucky;* ⓘ orcid.org/0000-0003-3012-5261

Mark R. Wiesner − *Center for the Environmental Implications of Nanotechnology, Durham, North Carolina, and Duke University, Durham, North Carolina;* ⓘ orcid.org/0000-0001-7152-7852

Complete contact information is available at:
https://pubs.acs.org/10.1021/acs.est.9b05097

Notes
The authors declare no competing financial interest.

■ REFERENCES

(1) Ferry, J. L.; Craig, P.; Hexel, C.; Sisco, P.; Frey, R.; Pennington, P. L.; Fulton, M. H.; Scott, I. G.; Decho, A. W.; Kashiwada, S.; Murphy, C. J.; Shaw, T. J. Transfer of Gold Nanoparticles from the Water Column to the Estuarine Food Web. *Nat. Nanotechnol.* **2009**, *4*, 441−444.

(2) Lowry, G. V.; Espinasse, B. P.; Badireddy, A. R.; Richardson, C. J.; Reinsch, B. C.; Bryant, L. D.; Bone, A. J.; Deonarine, A.; Chae, S.; Therezien, M.; Colman, B. P.; Hsu-Kim, H.; Bernhardt, E. S.; Matson, C. W.; Wiesner, M. R. Long-Term Transformation and Fate of Manufactured Ag Nanoparticles in a Simulated Large Scale Freshwater Emergent Wetland. *Environ. Sci. Technol.* **2012**, *46*, 7027−7036.

(3) Auffan, M.; Masion, A.; Mouneyrac, C.; de Garidel Thoron, C.; Hendren, C. O.; Thiery, A.; Santaella, C.; Giamberini, L.; Bottero, J.-Y.; Wiesner, M. R.; Rose, J. Contribution of Mesocosm Testing to a Single-Step and Exposure-Driven Environmental Risk Assessment of Engineered Nanomaterials. *NanoImpact* **2019**, *13*, 66−69.

(4) Baker, L. F.; King, R. S.; Unrine, J. M.; Castellon, B. T.; Lowry, G. V.; Matson, C. W. Press or Pulse Exposures Determine the Environmental Fate of Cerium Nanoparticles in Stream Mesocosms. *Environ. Toxicol. Chem.* **2016**, *35*, 1213−1223.

(5) Colman, B. P.; Baker, L. F.; King, R. S.; Matson, C. W.; Unrine, J. M.; Marinakos, S. M.; Gorka, D. E.; Bernhardt, E. S. Dosing, Not the Dose: Comparing Chronic and Pulsed Silver Nanoparticle Exposures. *Environ. Sci. Technol.* **2018**, DOI: 10.1021/acs.est.8b01700.

(6) Kulacki, K. J.; Cardinale, B. J.; Keller, A. A.; Bier, R.; Dickson, H. How Do Stream Organisms Respond to, and Influence, the Concentration of Titanium Dioxide Nanoparticles? A Mesocosm Study with Algae and Herbivores. *Environ. Toxicol. Chem.* **2012**, *31*, 2414−2422.

(7) Bour, A.; Mouchet, F.; Cadarsi, S.; Silvestre, J.; Verneuil, L.; Baqué, D.; Chauvet, E.; Bonzom, J.-M.; Pagnout, C.; Clivot, H.; Fourquaux, I.; Tella, M.; Auffan, M.; Gauthier, L.; Pinelli, E. Toxicity of CeO2 Nanoparticles on a Freshwater Experimental Trophic Chain: A Study in Environmentally Relevant Conditions through the Use of Mesocosms. *Nanotoxicology* **2016**, *10*, 245−255.

(8) Tella, M.; Auffan, M.; Brousset, L.; Morel, E.; Proux, O.; Chanéac, C.; Angeletti, B.; Pailles, C.; Artells, E.; Santaella, C.; Rose, J.; Thiéry, A.; Bottero, J.-Y. Chronic Dosing of a Simulated Pond Ecosystem in Indoor Aquatic Mesocosms: Fate and Transport of CeO$_2$ Nanoparticles. *Environ. Sci. Nano* **2015**, *2*, 653−663.

(9) Lead, J. R.; Batley, G. E.; Alvarez, P. J. J.; Croteau, M.-N.; Handy, R. D.; McLaughlin, M. J.; Judy, J. D.; Schirmer, K. Nanomaterials in the Environment: Behavior, Fate, Bioavailability, and Effects-An Updated Review. *Environ. Toxicol. Chem.* **2018**, *37*, 2029−2063.

(10) Levard, C.; Doelsch, E.; Basile-Doelsch, I.; Abidin, Z.; Miche, H.; Masion, A.; Rose, J.; Borschneck, D.; Bottero, J.-Y. Structure and Distribution of Allophanes, Imogolite and Proto-Imogolite in Volcanic Soils. *Geoderma* **2012**, *183−184*, 100−108.

(11) Aiken, G. R.; Hsu-Kim, H.; Ryan, J. N. Influence of Dissolved Organic Matter on the Environmental Fate of Metals, Nanoparticles, and Colloids. *Environ. Sci. Technol.* **2011**, *45*, 3196−3201.

(12) Dale, A. L.; Casman, E. A.; Lowry, G. V.; Lead, J. R.; Viparelli, E.; Baalousha, M. Modeling Nanomaterial Environmental Fate in Aquatic Systems. *Environ. Sci. Technol.* **2015**, *49*, 2587−2593.

(13) Lowry, G. V.; Gregory, K. B.; Apte, S. C.; Lead, J. R. Transformations of Nanomaterials in the Environment. *Environ. Sci. Technol.* **2012**, *46*, 6893−6899.

(14) Unrine, J. M.; Colman, B. P.; Bone, A. J.; Gondikas, A. P.; Matson, C. W. Biotic and Abiotic Interactions in Aquatic Microcosms Determine Fate and Toxicity of Ag Nanoparticles. Part 1. Aggregation and Dissolution. *Environ. Sci. Technol.* **2012**, *46*, 6915−6924.

(15) Avellan, A.; Simonin, M.; McGivney, E.; Bossa, N.; Spielman-Sun, E.; Rocca, J. D.; Bernhardt, E. S.; Geitner, N. K.; Unrine, J. M.; Wiesner, M. R.; Lowry, G. V. Gold Nanoparticle Biodissolution by a Freshwater Macrophyte and Its Associated Microbiome. *Nat. Nanotechnol.* **2018**, *13*, 1072−1077.

(16) Ellis, L.-J. A.; Baalousha, M.; Valsami-Jones, E.; Lead, J. R. Seasonal Variability of Natural Water Chemistry Affects the Fate and Behaviour of Silver Nanoparticles. *Chemosphere* **2018**, *191*, 616−625.

(17) Schlesinger, W. H.; Bernhardt, E. S.; Schlesinger, W. H.; Bernhardt, E. S. *Biogeochemistry*; Academic Press, 2013.

(18) Smith, V. H.; Tilman, G. D.; Nekola, J. C. Eutrophication: Impacts of Excess Nutrient Inputs on Freshwater, Marine, and Terrestrial Ecosystems. *Environ. Pollut.* **1999**, *100*, 179−196.

(19) Simonin, M.; Colman, B. P.; Anderson, S. M.; King, R. S.; Ruis, M. T.; Avellan, A.; Bergemann, C. M.; Perrotta, B. G.; Geitner, N. K.; Ho, M.; de la Barrera, B.; Unrine, J. M.; Lowry, G. V.; Richardson, C. J.; Wiesner, M. R.; Bernhardt, E. S. Engineered Nanoparticles Interact with Nutrients to Intensify Eutrophication in a Wetland Ecosystem Experiment. *Ecol. Appl.* **2018**, *28*, 1435−1449.

(20) Espinasse, B. P.; Geitner, N. K.; Schierz, A.; Therezien, M.; Richardson, C. J.; Lowry, G. V.; Ferguson, L.; Wiesner, M. R. Comparative Persistence of Engineered Nanoparticles in a Complex Aquatic Ecosystem. *Environ. Sci. Technol.* **2018**, *52*, 4072−4078.

(21) Baalousha, M.; Cornelis, G.; Kuhlbusch, T. A. J.; Lynch, I.; Nickel, C.; Peijnenburg, W.; van den Brink, N. W. Modeling Nanomaterial Fate and Uptake in the Environment: Current Knowledge and Future Trends. *Environ. Sci. Nano* **2016**, *3*, 323−345.

(22) Geitner, N. K.; Bossa, N.; Wiesner, M. R. Formulation and Validation of a Functional Assay-Driven Model of Nanoparticle Aquatic Transport. *Environ. Sci. Technol.* **2019**, *53*, 3104−3109.

(23) Luoma, S. N.; Khan, F. R.; Croteau, M.-N. Bioavailability and Bioaccumulation of Metal-Based Engineered Nanomaterials in Aquatic Environments: Concepts and Processes. *Front. Nanosci.* **2014**, *7*, 157−193.

(24) Vencalek, B. E.; Laughton, S. N.; Spielman-Sun, E.; Rodrigues, S. M.; Unrine, J. M.; Lowry, G. V.; Gregory, K. B. In Situ Measurement of CuO and Cu(OH)2 Nanoparticle Dissolution Rates in Quiescent Freshwater Mesocosms. *Environ. Sci. Technol. Lett.* **2016**, *3*, 375−380.

(25) Pourbaix, M. *Atlas of Electrochemical Equilibria in Aqueous Solutions*; Pergamon Press, 1966; Vol. *1*.

(26) Geitner, N. K.; Cooper, J. L.; Avellan, A.; et al. Size-Based Differential Transport, Uptake, and Mass Distribution of Ceria (CeO2) Nanoparticles in Wetland Mesocosms. *Environ. Sci. Technol.* **2018**, *52*, 9768−9776.

(27) Turkevich, J.; Stevenson, P. C.; Hillier, J. A Study of the Nucleation and Growth Processes in the Synthesis of Colloidal Gold. *Discuss. Faraday Soc.* **1951**, *11*, 55.

(28) *Safety Data Sheet Kocide 3000 Fungicide/Bactericide*, version 2.0; DuPont, 2015.

(29) Kah, M.; Navarro, D.; Kookana, R. S.; Kirby, J. K.; Santra, S.; Ozcan, A.; Kabiri, S. Impact of (Nano)Formulations on the Distribution and Wash-off of Copper Pesticides and Fertilisers Applied on Citrus Leaves. *Environ. Chem.* **2019**, *401*.

(30) Kah, M.; Kookana, R. S.; Gogos, A.; Bucheli, T. D. A Critical Evaluation of Nanopesticides and Nanofertilizers against Their Conventional Analogues. *Nat. Nanotechnol.* **2018**, *13*, 677−684.

(31) Li, J.; Rodrigues, S.; Tsyusko, O. V.; Unrine, J. M. Comparing Plant−Insect Trophic Transfer of Cu from Lab-Synthesised Nano-Cu(OH)2 with a Commercial Nano-Cu(OH)2 Fungicide Formulation. *Environ. Chem.* **2019**, *411*.

(32) Kirchner, J. *Data Analysis Toolkit: Uncertainty Analysis and Error Propagation*, 2001.

(33) Gustafsson, J. *Visual MINTEQ*, version 3.1; KTH Department of Land and Water Resources: Stockholm, Sweden, 2013. Based on de Allison, J. D.; Brown, D. S.; Novo-Gradac, K. J. *MINTEQA2*, version 2011,4, 1991.

(34) van Schaik, J. W. J.; Kleja, D. B.; Gustafsson, J. P. Acid−Base and Copper-Binding Properties of Three Organic Matter Fractions Isolated from a Forest Floor Soil Solution. *Geochim. Cosmochim. Acta* **2010**, *74*, 1391−1406.

(35) Sjöstedt, C. S.; Gustafsson, J. P.; Köhler, S. J. Chemical Equilibrium Modeling of Organic Acids, PH, Aluminum, and Iron in Swedish Surface Waters. *Environ. Sci. Technol.* **2010**, *44*, 8587−8593.

(36) Kalbitz, K.; Geyer, S.; Geyer, W. A Comparative Characterization of Dissolved Organic Matter by Means of Original Aqueous Samples and Isolated Humic Substances. *Chemosphere* **2000**, *40*, 1305−1312.

(37) Alberts, J. J.; Dickson, T. J. Organic Carbon and Cation Associations in Humic Material from Pond Water and Sediment. *Org. Geochem.* **1985**, *8*, 55−64.

(38) Webb, S. M. SIXPack a Graphical User Interface for XAS Analysis Using IFEFFIT. *Phys. Scr.* **2005**, *2005*, 1011.

(39) Ravel, B.; Newville, M. *ATHENA, ARTEMIS, HEPHAESTUS*: Data Analysis for X-Ray Absorption Spectroscopy Using *IFEFFIT*. *J. Synchrotron Radiat.* **2005**, *12*, 537−541.

(40) Andersen, M. R.; Kragh, T.; Sand-Jensen, K. Extreme Diel Dissolved Oxygen and Carbon Cycles in Shallow Vegetated Lakes. *Proc. R. Soc. B* **2017**, *284*, No. 20171427.

(41) Jones, J. I.; Hardwick, K.; Eaton, J. W. Diurnal Carbon Restrictions on the Photosynthesis of Dense Stands of *Elodea nuttallii* (Planch.) St. John. *Hydrobiologia* **1996**, *340*, 11−16.

(42) Kragh, T.; Andersen, M. R.; Sand-Jensen, K. Profound Afternoon Depression of Ecosystem Production and Nighttime Decline of Respiration in a Macrophyte-Rich, Shallow Lake. *Oecologia* **2017**, *185*, 157−170.

(43) Van den Berg, M. S.; Coops, H.; Simons, J.; Pilon, J. A Comparative Study of the Use of Inorganic Carbon Resources by Chara Aspera and Potamogeton Pectinatus. *Aquat. Bot.* **2002**, *72*, 219−233.

(44) Madsen, T. V.; Sand-Jensen, K. Photosynthetic Carbon Assimilation in Aquatic Macrophytes. *Aquat. Bot.* **1991**, *41*, 5−40.

(45) Cory, R. M.; Harrold, K. H.; Neilson, B. T.; Kling, G. W. Controls on Dissolved Organic Matter (DOM) Degradation in a Headwater Stream: The Influence of Photochemical and Hydrological Conditions in Determining Light-Limitation or Substrate-Limitation of Photo-Degradation. *Biogeosciences* **2015**, *12*, 6669−6685.

(46) Haramoto, T.; Ikusima, I. Life Cycle of *Egeria densa* Planch., an Aquatic Plant Naturalized in Japan. *Aquat. Bot.* **1988**, *30*, 389−403.

(47) Breault, R. F.; Colman, J. A.; Aiken, G. R.; McKnight, D. Copper Speciation and Binding by Organic Matter in Copper-Contaminated Streamwater. *Environ. Sci. Technol.* **1996**, *30*, 3477−3486.

(48) Klaine, S. J.; Alvarez, P. J. J.; Batley, G. E.; Fernandes, T. F.; Handy, R. D.; Lyon, D. Y.; Mahendra, S.; McLaughlin, M. J.; Lead, J. R. Nanomaterials in the Environment: Behavior, Fate, Bioavailability, and Effects. *Environ. Toxicol. Chem.* **2008**, *27*, 1825−1851.

(49) Yruela, I. Copper in Plants. *Braz. J. Plant Physiol.* **2005**, *17*, 145−156.

(50) King, R. S.; Richardson, C. J. Subsidy−Stress Response of Macroinvertebrate Community Biomass to a Phosphorus Gradient in an Oligotrophic Wetland Ecosystem. *J. North Am. Benthol. Soc.* **2007**, *26*, 491−508.

(51) Pietrobelli, J. M. T. d. A.; Módenes, A. N.; Fagundes-Klen, M. R.; Espinoza-Quiñones, F. R. Cadmium, Copper and Zinc Biosorption Study by Non-Living *Egeria densa* Biomass. *Water, Air, Soil Pollut.* **2009**, *202*, 385−392.

(52) Global Invasive Species Database (GISD). *Species Profile: Egeria densa. Invasive Species*; GISD, 2018.

(53) Arnesano, F.; Banci, L.; Bertini, I.; Mangani, S.; Thompsett, A. R. A Redox Switch in CopC: An Intriguing Copper Trafficking Protein That Binds Copper(I) and Copper(II) at Different Sites. *Proc. Natl. Acad. Sci.* **2003**, *100*, 3814−3819.

(54) Stegemeier, J. P.; Avellan, A.; Lowry, G. V. Effect of Initial Speciation of Copper- and Silver-Based Nanoparticles on Their Long-Term Fate and Phytoavailability in Freshwater Wetland Mesocosms. *Environ. Sci. Technol.* **2017**, *51*, 12114−12122.

(55) Bohu, T.; Anand, R.; Noble, R.; Lintern, M.; Kaksonen, A. H.; Mei, Y.; Cheng, K. Y.; Deng, X.; Veder, J.-P.; Bunce, M.; Power, M.; Verrall, M. Evidence for Fungi and Gold Redox Interaction under Earth Surface Conditions. *Nat. Commun.* **2019**, *10*, No. 2290.

(56) MANN, K. H. Annual Fluctuations in Sulphate and Bicarbonate Hardness in Ponds. *Limnol. Oceanogr.* **1958**, *3*, 418−422.

(57) Westerhoff, P.; Nowack, B. Searching for Global Descriptors of Engineered Nanomaterial Fate and Transport in the Environment. *Acc. Chem. Res.* **2013**, *46*, 844−853.

(58) OECD. *Assessment of Biodurability of Nanomaterials and the Surface Ligands*; Series on the Safety of Manufactured Nanomaterials, No. 86; OECD, 2018.

(59) Levard, C.; Hotze, E. M.; Colman, B. P.; Dale, A. L.; Truong, L.; Yang, X. Y.; Bone, A. J.; Brown, G. E.; Tanguay, R. L.; Di Giulio, R. T.; Bernhardt, E. S.; Meyer, J. N.; Wiesner, M. R.; Lowry, G. V. Sulfidation of Silver Nanoparticles: Natural Antidote to Their Toxicity. *Environ. Sci. Technol.* **2013**, *47*, 13440−13448.

(60) Auffan, M.; Rose, J.; Bottero, J.-Y.; Lowry, G. V.; Jolivet, J.-P.; Wiesner, M. R. Towards a Definition of Inorganic Nanoparticles from an Environmental, Health and Safety Perspective. *Nat. Nanotechnol.* **2009**, *4*, 634−641.